



DOI: 10.5604/01.3001.0054.7241

Pulse frequency density modulation full bridge for induction preheating application of stainless-steel welding

P. Chakkuchan ^a, S. Chudjuarjeen ^{a,*}, N. Phankong ^b

^a Department of Electrical Engineering, Faculty of Engineering, Rajamangala University of Technology Krungthep, 10120 Bangkok, Thailand

^b Department of Electrical Engineering, Faculty of Engineering, Rajamangala University of Technology Thanyaburi, 12110 Pathum Thani, Thailand

* Corresponding e-mail address: saichol.c@mail.rmutk.ac.th

ORCID identifier:  <https://orcid.org/0000-0003-4819-4273> (S.C.)

ABSTRACT

Purpose: The paper shows the problem of surface cracks from welding (TIG welding) to welding stainless steel pipe (heat-affected zone: HAZ). The study is an experiment of preparing welding with non-heating workpieces and preheating the workpiece using the principle of induction, heating with a fluid inverter circuit that can adjust power by frequency control, pulse frequency density modulation (PFDM) to maintain temperature for industrial.

Design/methodology/approach: The control circuit is responsible for regulating the functioning of different devices and the speed of operation of the switch device. It divides the control into two closed loops: phase-angle feedback and current feedback. The phase-angle feedback loop ensures frequency tracking during the phase check angle, enabling the inverter to operate at frequencies higher than the resonant frequency throughout its operation. The process of arc welding was employed in the fusion of stainless-steel materials. Preheating is a crucial step in the welding process, as it serves to uphold the integrity of the weld and mitigate the occurrence of undesirable outcomes such as cracking and the subsequent requirement for rework. The Welding Process Specification (WPS) about the task at hand will delineate the lower and upper limits of preheating temperatures and the requisite period for preheating. High-quality products should be devoid of these imperfections and possess comprehensive welding reinforcement. Additional welding certifications encompassed a tensile testing procedure, a microhardness testing procedure, and a comprehensive microstructure analysis.

Findings: Applying an alternating voltage to an induction coil generates an alternating current (AC) within the coil circuit. The induced currents exhibit a frequency identical to that of the coil current, although they possess an opposite direction to the coil current. These currents facilitate heat generation through the phenomenon known as the Joule effect. The temperature range of 250°C–400°C can be effectively regulated for preheating stainless steel by using high-frequency electric process heating in induction welding, hence achieving the desired welding preheat. There are two primary classifications for inverters: voltage-source inverters and current-source inverters.

Research limitations/implications: The main research limitation is comparing preheat and non-preheat. The size of the heat-affected zones is influenced by the rate of heating and cooling brought on by machining processes. By influencing the microstructural changes in that area,



precise control of the variables can impact the integrity of the weld zones. The microstructural characteristics of the metal are different from the rest of the subject because welding heats the metal. The topic is heated up beforehand to ensure smooth welding and structural integrity. Because there is less of a temperature difference between the weld zone and the base material, preheating during welding results in less shrinkage stress. Distortions and crack flaws might result from higher shrinkage stress.

Practical implications: NDT, or non-destructive testing, is a weld integrity test to find defects that occur in the weld without damaging that welding line and continuing to use it safely. For the welding line to be strong according to the design of that welding line (conformance to design), the test will use the principles of physical properties, such as light, X or gamma rays, magnetic fields, and high-frequency sound waves.

Originality/value: In the research, stainless steel was successfully welded to preheat using induction heating (IH).

Keywords: Stainless steel, Arc welding, Induction heating (IH), Heat affected zone (HAZ), Power electronics, Inverter voltage-source

Reference to this paper should be given in the following way:

P. Chakkuchan, S. Chudjuarjeen, N. Phankong, Pulse frequency density modulation full bridge for induction preheating application of stainless-steel welding, Archives of Materials Science and Engineering 127/1 (2024) 23-31. DOI: <https://doi.org/10.5604/01.3001.0054.7241>

MATERIALS MANUFACTURING AND PROCESSING

1. Introduction

Stainless steel is an alloy between steel and many substances; the most important is chromium, at least 10%, which can resist corrosion and rust. Both are from nature and are made in the environment. Stainless steel can be divided into more than 150 types but can also be divided into 8 groups, depending on the mixture of elements that make it have some different properties. The selection must be based on the properties and suitability of the job. The main differences are as follows:

- chromium is the main ingredient that gives steel the ability to resist rust and various forms of corrosion.
- nickel enhances rust resistance. and make stainless steel magnetic.
- molybdenum makes stainless steel more resistant to rust and chemicals such as chlorine.
- carbon is a hardening agent for stainless steel. If there is less carbon, Stainless steel will be more ductile instead.

Stainless steel products are widely used due to their special characteristics [1-3] that differ from those of other materials, such as good corrosion resistance and mechanical properties [4-5]. It can be used at high temperatures, has a smooth surface appearance, and has a wide range. Stainless steel is used not only for kitchenware, sanitary ware, and decoration but also for welding and assembly of pressure vessel pipes, tanks, and automobile exhaust systems. Stainless steel welding is different from austenitic welding and ferritic welding as the hard and brittle martensite structure [6] has the potential to crack if used immediately.

Without preheating and post-heat treatment, the risk of cracking increases as the carbon content increases (Fig. 1). The above problems can be mitigated by preheating to a temperature of about 200-300°C and controlling the heat input and interpass temperature to facilitate uniform weld cooling and reduce stresses. In addition to reducing the risk of cracking in the weld, another problem that may be encountered is that cracks caused by hydrogen embrittlement can be prevented by choosing a welding process with hydrogen in flux. Stainless steel, or stainless steel in metallurgy, is considered an alloy of steel. With at least 10.5% chromium, the alloy does not rust due to the reaction between oxygen in the air and chromium in meat.



Fig. 1. The use of gas fire to heat the surface of the workpiece

Stainless steel forms a thin film on the surface. It also serves to protect against damage to the stainless steel. The type of stainless steel is classified as commercial grade, which is generally available and easy to find. It is often used to make general appliances. We can classify the type of stainless steel from the code number established according to the AISI standard, such as 304, 304L, 316, 316L, etc., in which the mixture determines the grade of stainless steel, which has different usage requirements. Stainless and rusting stainless steel usually does not rust because its surface has a chromium oxide film. A thin coating on the surface is due to the reaction between Cr in stainless steel and oxygen in the air. The destruction of the chromium oxide film causes stainless steel rust. It is coated in a condition where stainless steel can rust before the chromium oxide film forms again, e.g., If the stainless steel is scratched, Then the area has moisture, which can cause a reaction with iron before the chromium oxide film is formed. It will cause rust to occur.

All stainless steel has much lower thermal conductivity than carbon steel. The thermal conductivity of plain chromium steel is $\frac{1}{3}$, and carbon steel's austenitic grade is $\frac{1}{4}$. It affects its use at high temperatures; for example, it affects the amount of heat input during welding, requiring a longer heating period. when working with hot forming. Austenitic group Also known as "Series 300," approximately 70% of the world's stainless-steel production is austenitic stainless steel. It contains at least 0.15% carbon, at least 16% chromium, and nickel, which improves Features of formability and increased corrosion resistance. Some grades contain manganese as well. It generally contains 18 per cent chromium and 10 per cent nickel and is often referred to as 18/10, like 18/0 and 18/8, such as grades 304, 304L and S32654. Kitchenware applications: Tableware, food and electrical appliances, building decoration, architecture, beer production equipment, or food and beverage products with resistance properties related to cleanliness and hygiene, such as hospital equipment and pharmaceuticals, can be used at negative temperatures. Liquefied gas storage tanks can be used at high temperatures, as can heat exchanger pipes. Making equipment for controlling or eliminating pollution and toxic fumes, pipework, storage tanks, containers used in industry, and container pressure are used in the chemical, petrochemical, and petroleum product industries—mining industry production of tissue paper and paper equipment in train carriages, carts, and food.

Additionally, flame preheating presents safety risks, such as an elevated burn potential, and has unique storage needs for explosive gases, most frequently propane or propylene. Preheating can also be done in an oven or

furnace, especially for small items. Huge models are available for big weldments. Induction heating is frequently used for pipe welding [7,8] and is a safe choice for pre and post-weld heat treating (PWHT). Induction heating systems produce localized eddy currents within a conductive part. An alternating current is used to achieve this by running it through a coil placed extremely close to or around the component. As a result, the part experiences eddy currents due to the alternating magnetic fields that are created close to the coil. The component heats up quickly because of the material's intrinsic resistance to this current, thus acting as its own heating element. It is a particularly efficient technology because it eliminates or significantly reduces the heat loss common with other heating techniques. The interpass temperature refers to the temperature that exists between successive weld passes. Maintaining a consistent interpass temperature for multi-pass welds is of utmost importance, as it should align with the preheat temperature or be determined by the code, material specification, or welding process specification (WPS). Maintaining uniform preheat temperature across each weld pass is imperative to provide consistent hydrogen deposition, composition, and cooling capacity in all deposited weld metal lines. The reduction of stresses and the facilitation of hydrogen diffusion are achieved by implementing the minimum interpass temperature, commonly referred to as the preheat temperature.

The half-bridge and class D resonant inverter for high voltage in the context of induction heating applications. Variable-frequency duty cycles of square wave pulse-frequency modulation (PFM) are often utilized approaches for controlling the output power in the majority of induction heating (IH) applications [3, 9-11]. The utilization of frequency modulation control is a prevalent practice in mitigating fluctuations in load or line frequency. However, the implementation of frequency modulation control poses several obstacles since it requires the adjustment of the switching frequency across a wide range to effectively handle various load and line combinations that are particularly unfavourable. Moreover, while operating below resonance, the dimensions of filter components expand due to the requirement to build them for the low-frequency range. In addition, the operation of many inverters with different switching frequencies will probably result in an audible sound. Furthermore, it is important to acknowledge that the effective range of the zero-voltage switching (ZVS)-PFM high-frequency inverter is slightly restricted when utilizing a pulse frequency modulation (PFM) technique [12,13].

The paper proposes power adjustment control. By means of adjusting the density of the pulse width modulation contract. At the switch, the driving signal of the full bridge

inverter circuit for heating stainless steel pipes and has the results of simulating the operation of the circuit. To know the coordinates of the equipment used and compare them with the theoretically consistent actual experimental results. The prototype uses an AC voltage system on the input side of 230V/50 Hz with an input power of 1 kW, operating at a resonance frequency of 57-65 kHz. The power on the output side can be adjusted as well.

1.1. Series resonant inverter

The induction inverter offered consists of 220V, AC voltage supply, and 50 Hz frequency with L_{DC1} inductor. In the section of the resonance circuit, the full bridge inverter includes a Q_1, Q_2, Q_3, Q_4 power switch, L_{coil} resonant inductor, and Cr resonant capacitor in the proposed circuit Figure 2.

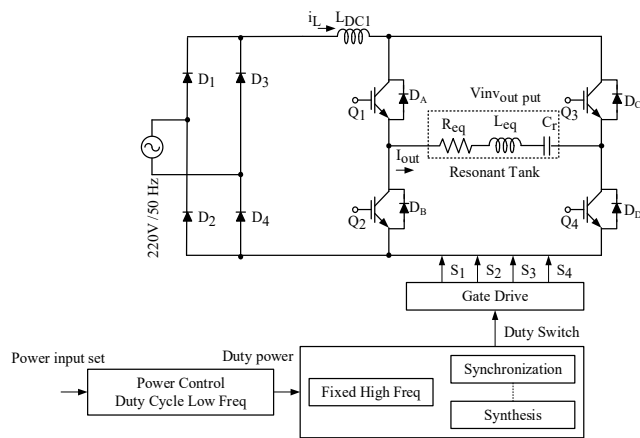


Fig. 2. Proposed control block diagram full-bridge inverter

The definition of the natural resonance frequency is provided by Equation (1).

$$\omega_r = \frac{1}{\sqrt{L_{eq} \cdot C_r}} \quad (1)$$

$$\text{Skin depth, } \delta = \sqrt{\frac{\rho}{\mu f \pi}} \quad (2)$$

by
 δ is surface depth (m),
 ρ is a specification of workpiece resistance (Ωm),
 μ is magnetic dispersion of workpieces (H/m),
 f is frequency of switching power supply (Hz).

1.2. Operation mode of inverter full-bridge

Waveforms sketched in Figure 3. The full-bridge inverter, covering the switching signals, resonant tank

voltage V_{S2} and load current i_{Leq} . Based on the information presented in Figure 4, it can be observed that the series-resonant circuit exhibits the characteristics of an inductive load when the switches are engaged at frequencies that surpass the resonant frequency. In the above scenario, the magnitude of the load current i_{Leq} is affected by the voltage across the tank. Therefore, the current carrying capacity is divided between two components.

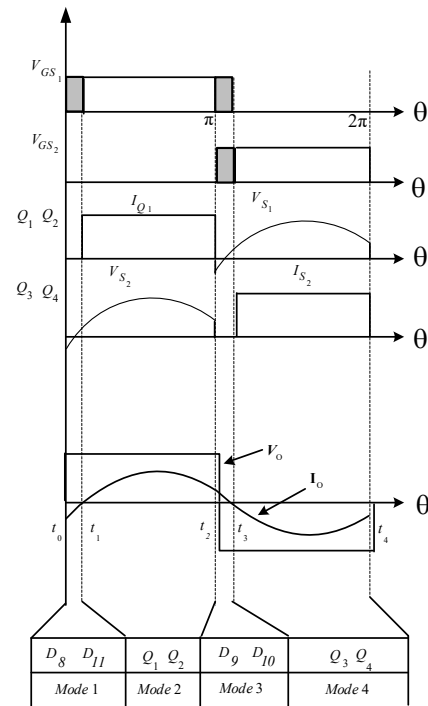


Fig. 3. Waveforms in the inverter full bridge 4 mode operation circuit

The input impedance of the resonant tank is given by.

$$Z_{eq} = R_{eq} + j \left(\omega_s L_{eq} - \frac{1}{\omega_s C_r} \right) \quad (3)$$

$$Z_{eq} = R_{eq} \cdot \left(1 + j Q_L \cdot \left(\omega_n - \frac{1}{\omega_n} \right) \right) \quad (4)$$

The input voltage can determine the voltage applied to the resonant tank.

$$V_{S2} = V_m \cdot \sin \omega_s t, \text{ for } 0 < \omega_s t \leq 2\pi \quad (5)$$

The amplitude of voltage is given by.

$$V_m = \frac{4 \cdot V_s}{\pi} \approx 1.273 \cdot V_s. \quad (6)$$

The determination of the load current passing through the resonant tank is calculated using.

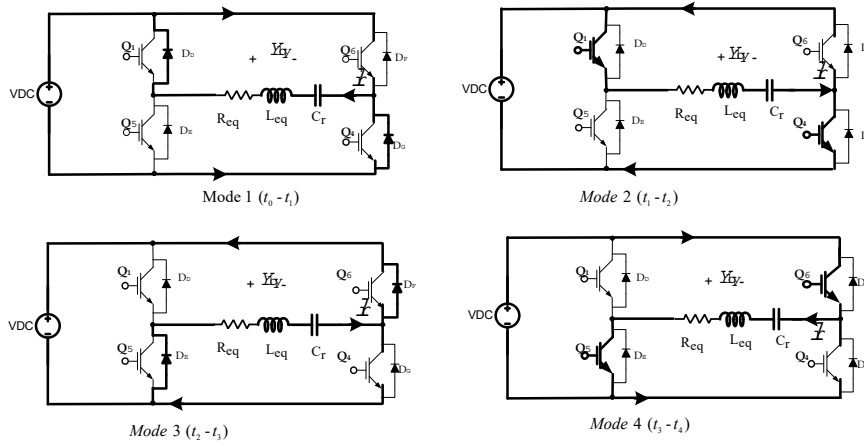


Fig. 4. Operation modes of full-bridge inverter

$$I_m = \frac{V_m}{|Z_{eq}|} \tag{7}$$

$$I_m = \frac{4 \cdot V_d}{\pi \cdot |Z_{eq}|} \tag{8}$$

$$I_m = \frac{4 \cdot V_d \cdot \cos \phi}{\pi \cdot R_{eq}} \tag{9}$$

$$I_m = \frac{4 \cdot V_d}{\pi \cdot R_{eq} \cdot \sqrt{1 + Q_L^2 \left(\frac{\omega}{\omega_0} - \frac{\omega_0}{\omega} \right)^2}} \tag{10}$$

The output power is obtained from (10).

$$P_{out} = I_m^2 \frac{R_{eq}}{2} \tag{11}$$

$$P_{out} = \frac{8 \cdot V_d^2 \cdot R_{eq} \cdot \cos^2 \phi}{\pi^2 \cdot R^2} \tag{12}$$

$$P_{out} = \frac{8 \cdot V_d^2 \cdot R_{eq}}{\pi^2 \cdot R^2 \cdot \sqrt{1 + Q_L^2 \left(\frac{\omega}{\omega_0} - \frac{\omega_0}{\omega} \right)^2}} \tag{13}$$

2. Simulation and experimental result

To simulate the process, the different parameter values that were found were used to figure out the induction cylinder and the switches' frequency values. So that the steady-state operation modelling can be used to figure out why the current circuit and the inverter are not working. The amount of pressure and power at different parts of the device in the circuit ensures the device does not go beyond what it is supposed to do. The article discusses the test results of the inverter and control circuits. The results show that different changes have been made by heating the stainless steel plate

and doing experiments. The workpiece is 6 cm × 30 cm long and heats workpieces for 10 cm.

Figure 5 shows a simulation of the operation of the circuit to find the pressure and current values that flow through the switch, to select the appropriate equipment. Do not overload.

Parameters for the hardware setup is shown in Table 1.

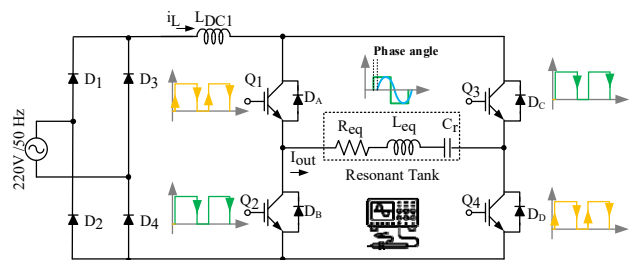


Fig. 5. Simulation control circuit for induction heating.

Table 1.

Parameters for the hardware setup

Item	Symbol	Value
Input voltage	V_{AC}	230 V_{rms}
Switching high frequency of full-bridge inverter	$f_{S_{high}}$	57 – 65 kHz
Switching low frequency for control	$f_{S_{low}}$	60 Hz
Induction coil	L_{eq}	1.85 mH
Load resistor	R_{eq}	25.6 $m\Omega$
Resonant capacitor	C_r	4 μF

Figure 6 shows a simulation output power fixed value of R_{eq} .

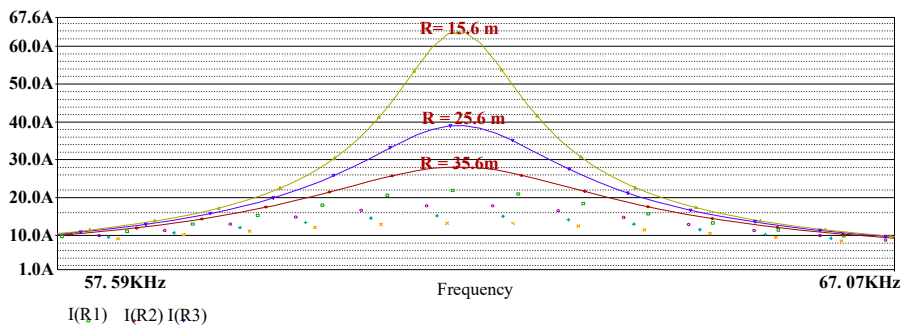


Fig. 6. Simulation output power fixed values of R_{eq}

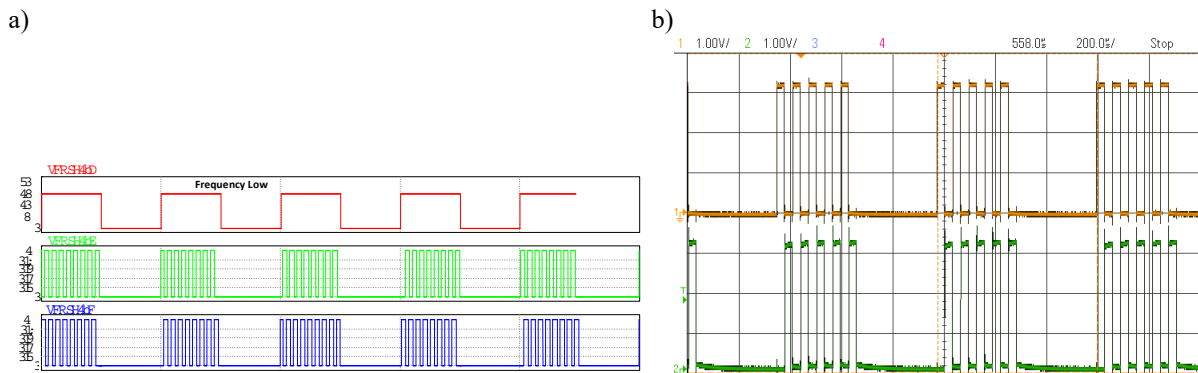


Fig. 7. a) Simulation waveforms of signal control, b) experimental waveforms of signal (high, low) at switching inverter

The result of calculating each resistance value, starting with R equal to $35.6\text{ m}\Omega$, will be the lowest current value in the circuit. Compared to R equal to $15.6\text{ m}\Omega$, the resonant circuit will obtain the highest current value.

Figure 7a shows simulation waveforms low-frequency and high-frequency for control power output at the inverter. Figure 7b shows a low-frequency signal waveform with 50% duty cycle adjustment – Figure 8 zooms in on the waveform rise-time switch inverter, and Figure 9 zooms in on the waveform fall-time switch inverter.

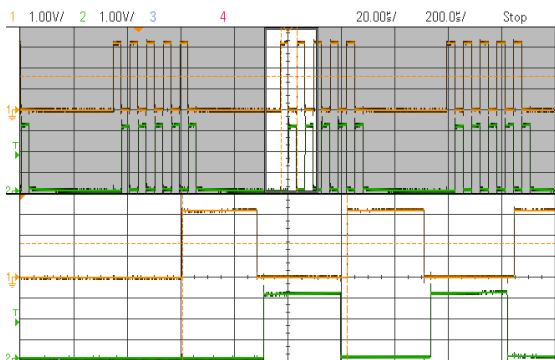


Fig. 8. Experimental waveforms signal (Q_1, Q_2) on time of $Duty_{power}$ (1V/Div, time $20\mu\text{s}/\text{Div}$)

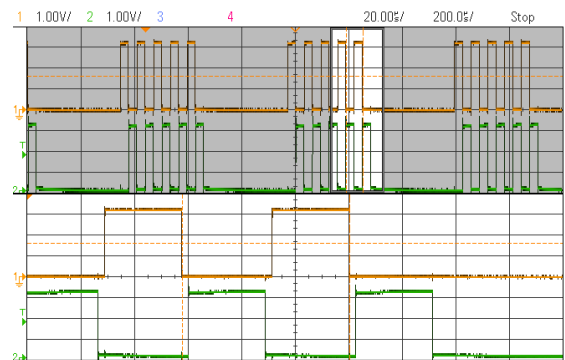


Fig. 9. Experimental waveforms signal (Q_1, Q_2) off time of $Duty_{power}$ (1V/Div, time $20\mu\text{s}/\text{Div}$)

Figure 10 (signal zoom) shows experimental waveforms signal (V_{inv}, i_{inv}) adjust $Duty_{power} = 90\%$. Figure 11 in the testing of the side-adjustable power control set, the input converter set with low-frequency induction heating, which is the power regulator by recycling adjustment, must be able to be recycled, with frequencies are approximately 60 Hz. The high-frequency set maintains the desired frequency by making the high-frequency adjustments to 60.00 kHz. Figure 12 shows design induction coil length heat zone 10 cm work

piece diameter 6 cm. In Figure 13, room temperature workpiece and heating coil. Figure 14 a high temperature workpiece and heating coil are at 408°C.

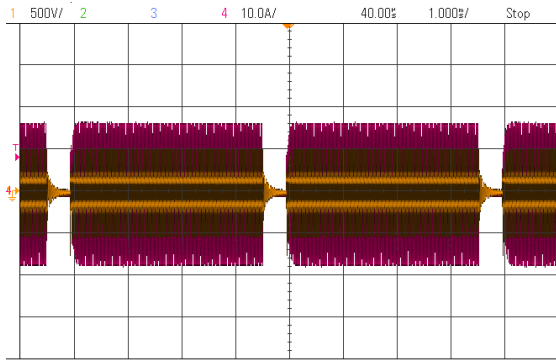


Fig. 10. Experimental waveforms signal (V_{inv} , i_{inv}) adjust $Duty_{power} = 90\%$

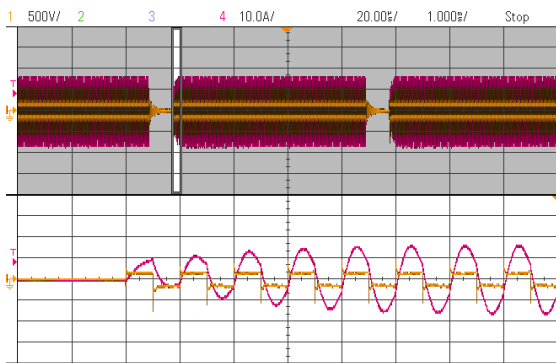


Fig. 11. Experimental waveforms signal zoom (V_{inv} , i_{inv}) adjust $Duty_{power} = 90\%$

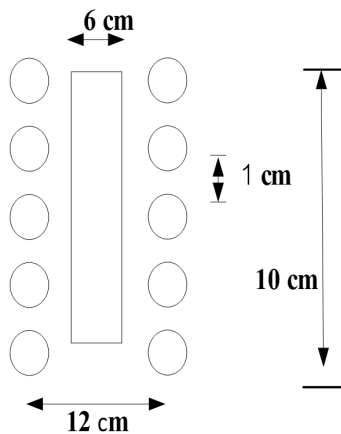


Fig. 12. Induction coil designed for stainless steel pipe heating



Fig. 13 Experimental stainless steel pipe and induction coil at room temperature

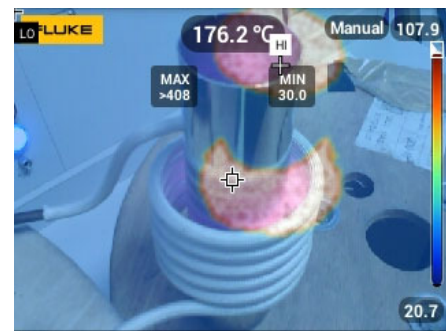


Fig. 14 Experimental stainless-steel pipe and induction coil at a temperature of 408°C

Find the equation efficiency of the inverter.

$$Efficiency = \frac{Output}{Input} \times 100\% \quad (14)$$

$$Efficiency = \frac{800W}{1,000W} \times 100\% = 80\%$$

3. Conclusions

The scope of this study encompasses the conceptualisation and development of a prototype for an induction heating apparatus. An inverter module is employed to assess the thermal behaviour of stainless-steel pipes before welding. The inverter module comprises a direct current voltage source, which is utilised to both bring the inverter module and regulate its functioning simultaneously. The topic of discussion pertains to half-bridge inverters and impedance adjustment transformers. The operational control can be categorized into two closed loops: an inner loop that is phase-locked and a frequency-tracking loop that enables the inverter to operate with a constant voltage phase angle leading the current. The purpose of the outer loop is to regulate the output power by manipulating the load current.

The experiment involved testing a prototype connected to a series of resonant loads. The load consisted of a stainless-steel object with dimensions of 12 cm in diameter and 10 cm in height.

Additionally, a set of inverter modules with a power capacity of 1 kW were connected to the load. This setup could generate temperatures ranging from 100–400°C within approximately 1 minute when supplied with an input power of 1 kW. Consequently, the prototype has the potential to enhance power output. The device can generate an output power of 0.8 kW.

Research funding

The research was funded by a project called the “Thailand Science Research and Innovation” grant number 66A166000008.

Authors contribution

The percentage of the authors’ contribution to the article’s creation, P. Chakkuchan, S. Chudjuarjeen and N. Phankong conceived of the presented idea was 30%. P. Chakkuchan developed the theory and experimental design 40%. S. Chudjuarjeen verified the analytical methods and writing reviewing and editing 30%. All authors discussed the results and contributed to the final manuscript.

References

- [1] P.A. Lee, S. Kim, B. Stakenborghs, Y. Suh, S. Choi, Development of hydro axial tension method for whole pipe butt-fusion joint tensile test, *Polymer Testing* 109 (2022) 107553. DOI: <https://doi.org/10.1016/j.polymertesting.2022.107553>
- [2] Z. Garncarek, J. Idzik, Degree of heterogeneity of thermal field a method of evaluation, *International Journal of Heat and Mass Transfer* 35/11 (1992) 2769-2775. DOI: [https://doi.org/10.1016/0017-9310\(92\)90297-6](https://doi.org/10.1016/0017-9310(92)90297-6)
- [3] G. Thomas, V. Ramachandra, R. Gamesman, R. Vasudevan, Effect of pre- and post-weld heat treatments on the mechanical properties of electron beam welded Ti-6Al-4V alloy, *Journal of Materials Science* 28 (1993) 4892-4899. DOI: <https://doi.org/10.1007/BF00361152>
- [4] D.I. Tsamroh, P. Puspitasari, Andoko, A.A. Permasari, P.E. Setyawan, Optimization of multistage artificial aging parameters on Al-Cu alloy mechanical properties, *Journal of Achievements in Materials and Manufacturing Engineering* 87/2 (2018) 62-67. DOI: <https://doi.org/10.5604/01.3001.0012.2828>
- [5] L.A. Dobrzański, L.B. Dobrzański, A.D. Dobrzańska-Danikiewicz, Overview of conventional technologies using the powders of metals, their alloys and ceramics in Industry 4.0 stage, *Journal of Achievements in Materials and Manufacturing Engineering* 98/2 (2020) 56-85. DOI: <https://doi.org/10.5604/01.3001.0014.1481>
- [6] Y. Samart, C. Panithan, S. Chudjuarjeen, A. Sangswang, C. Koopai, An automatic half-bridge resonant inverter with a three#phase three-switch buck-type rectifier. Proceedings of the IEEE Energy Conversion Congress and Exposition, Atlanta, GA, 2010, 2172-2176. DOI: <https://doi.org/10.1109/ECCE.2010.5618282>
- [7] Andoko, Yanuar, P. Puspitasari, T.B. Ariestoni, The effects of artificial-aging temperature on tensile strength, hardness, microstructure, and fault morphology in AlSiMg, *Journal of Achievements in Materials and Manufacturing Engineering* 98/2 (2020) 49-55. DOI: <https://doi.org/10.5604/01.3001.0014.1480>
- [8] N. Phankong, J. Jittakort, P. Chakkuchan, S. Kitcharoenwat, V. Hathairatsiri, C. Wisassakwichai, S. Chudjuarjeen, Induction heating application using frequency control techniques for hot tensile testing, Proceedings of the 18th International Conference on Electrical Engineering/Electronics, Computer, Telecommunications, and Information Technology “ECTI-CON”, Chiang Mai, Thailand, 2021, 968-971. DOI: <https://doi.org/10.1109/ECTI-CON51831.2021.9454777>
- [9] P. Chakkuchan, S. Chudjuarjeen, N. Phankong, S. Dangeam, M. Nawong, P. Nintanavongsa, Full-Bridge Current#Source Inverter Using Pulse Density Control for Induction Preheating of Welding Application, Proceedings of the 25th International Conference on Electrical Machines and Systems “ICEMS”, Chiang Mai, Thailand, 2022, 1-4. DOI: <https://doi.org/10.1109/ICEMS56177.2022.9983285>
- [10] A.P. Mackwood, R.C. Crafer, Thermal modelling of laser welding and related processes: a literature review, *Optics and Laser Technology* 37/2 (2005) 99-115. DOI: <https://doi.org/10.1016/j.optlastec.2004.02.017>
- [11] C. Ekkaravarodome, P. Charoenwiangnuea, K. Jirasereamornkul, The simple temperature control for induction cooker based on Class-E resonant inverter, Proceedings of the 10th International Conference on Electrical Engineering/Electronics, Computer,

Telecommunications and Information Technology, Krabi, Thailand, 2013, 1-6.

DOI: <https://doi.org/10.1109/ECTICon.2013.6559634>

- [12] P. Charoenwiangnuea, C. Ekkaravarodome, I. Boonyaroonate, P. Thounthong, K. Jirasereeamornkul, Design of domestic induction cooker based on optimal operation Class-E inverter with parallel load network under large-signal excitation, Journal of

Power Electronics 17/4 (2017) 892-904. DOI: <https://doi.org/10.6113/JPE.2019.17.4.892>

- [13] J. Jittakort, A. Sangswang, S. Naetiladanon, C. Koompai, S. Chudjuarjeen, Full bridge resonant inverter using asymmetrical control with resonant frequency tracking for ultrasonic cleaning applications, Journal of Power Electronics 17/5 (2017) 1150-1159. DOI: <https://doi.org/10.6113/JPE.2017.17.5.1150>



© 2024 by the authors. Licensee International OCSCO World Press, Gliwice, Poland. This paper is an open-access paper distributed under the terms and conditions of the Creative Commons Attribution-NonCommercial-NoDerivatives 4.0 International (CC BY-NC-ND 4.0) license (<https://creativecommons.org/licenses/by-nc-nd/4.0/deed.en>).